Eur. Phys. J. A **15**, 69–73 (2002)
DOI 10.1140/epja/i2001-10228-6

THE EUROPEAN PHYSICAL JOURNAL A

Asymptotic normalization coefficients in nuclear astrophysics and structure

C.A. Gagliardi[1,a], A. Azhari[1], V. Burjan[2], F. Carstoiu[3], V. Kroha[2], A.M. Mukhamedzhanov[1], A. Sattarov[1], X. Tang[1], L. Trache[1], and R.E. Tribble[1]

[1] Cyclotron Institute, Texas A&M University, College Station, TX 77843, USA
[2] Institute for Nuclear Physics, Czech Academy of Sciences, Prague-Řež, Czech Republic
[3] Institute for Atomic Physics, Bucharest, Romania

Received: 21 March 2002 /
Published online: 31 October 2002 –

Abstract. The asymptotic normalization coefficient (ANC) for a nuclear system specifies the normalization of the tail of the nuclear overlap function. ANCs may be determined experimentally by measuring peripheral nuclear reactions. They may be used to calculate the astrophysical S-factors for radiative capture reactions at stellar energies and to determine the halo structure of loosely bound nuclei. A brief introduction to ANCs is given and applications to the $^7\mathrm{Be}(p,\gamma)^8\mathrm{B}$ and $^{11}\mathrm{C}(p,\gamma)^{12}\mathrm{N}$ reactions and the halo structure of ^{8}B are described.

PACS. 26.30.+k Nucleosynthesis in novae, supernovae and other explosive environments – 26.20.+f Hydrostatic stellar nucleosynthesis – 25.60.Je Transfer reactions – 25.60.Gc Breakup and momentum distributions

1 Introduction to ANCs

The asymptotic normalization coefficient (ANC) C for the nuclear system $A + p \leftrightarrow B$ specifies the amplitude of the tail of the overlap function of the bound state B in the two-body channel $(A\,p)$. We show that ANCs can be determined from measurements of peripheral proton transfer reactions or one-nucleon breakup reactions of loosely bound nuclei, and they may be used to calculate direct radiative capture reaction rates of astrophysical interest at stellar energies, to estimate the gamma widths of certain resonances, and to investigate nuclear halo structures.

Traditionally, spectroscopic factors have been obtained from DWBA analysis of proton transfer reactions. However, these spectroscopic factors have significant systematic uncertainties associated with the choice of proton single-particle orbitals in the initial and final nuclei. For peripheral transfer reactions, the ANC is better determined and is the more natural quantity to extract. Consider the proton transfer reaction $a + A \to c + B$, where $a = c + p$ and $A + p = B$. We can write the cross-section in the form [1]

$$\frac{\mathrm{d}\sigma}{\mathrm{d}\Omega} = \sum_{j_B j_a} (C^B_{Apl_Bj_B})^2 (C^a_{cpl_aj_a})^2 \frac{\sigma^{\mathrm{DW}}_{l_Bj_Bl_aj_a}}{b^2_{Apl_Bj_B} b^2_{cpl_aj_a}}, \qquad (1)$$

where $\sigma^{\mathrm{DW}}_{l_Bj_Bl_aj_a}$ is the reduced DWBA cross-section. The C's are the ANCs at the two vertices, and the b's are the ANCs of the bound-state proton wave functions in nuclei a and B. If the reaction under consideration is peripheral, the ratio in eq. (1) is independent of $b_{Apl_Bj_B}$ and $b_{cpl_aj_a}$. Thus for surface reactions, the cross section is best parametrized in terms of the product of the squares of the ANCs of the initial and final nuclei, $(C^B)^2(C^a)^2$.

The important advantage of this formulation is that, given the ANC, the rates of other peripheral nuclear reactions, such as direct radiative capture at astrophysical energies or one-nucleon breakup of loosely bound nuclei, may be calculated and peripheral nuclear properties, such as halo structures, may be determined. For example, fig. 1 shows a comparison between the experimental S-factors for $^{16}\mathrm{O}(p,\gamma)^{17}\mathrm{F}$ [2,3] to those determined from ANCs measured in the $^{16}\mathrm{O}(^3\mathrm{He},d)^{17}\mathrm{F}$ reaction [4]. The good agreement demonstrates that ANCs measured in peripheral nucleon transfer reactions may be used to predict direct radiative capture rates at astrophysical energies to better than 9%. Additional tests of the ANC technique may be found in [5,6]. The following sections describe three recent applications of the ANC technique.

2 ^{14}N(^{11}C, ^{12}N)^{13}C and ^{11}C(p, γ)^{12}N

First-generation stars were composed entirely of nuclei produced in the Big Bang. Thus, such stars could only

[a] e-mail: cggroup@comp.tamu.edu

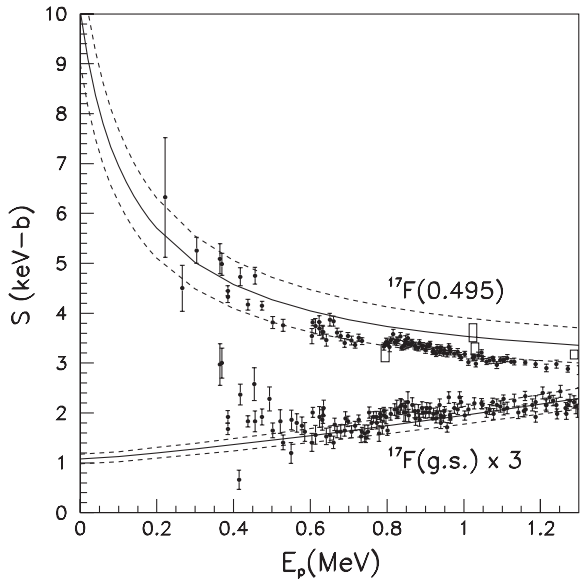

Fig. 1. A comparison of the experimental S-factors for $^{16}\mathrm{O}(p,\gamma)^{17}\mathrm{F}$ to those determined from the ANCs found in $^{16}\mathrm{O}(^3\mathrm{He},d)^{17}\mathrm{F}$. The solid curves are the calculated S-factors and the dashed curves show 1σ error bands.

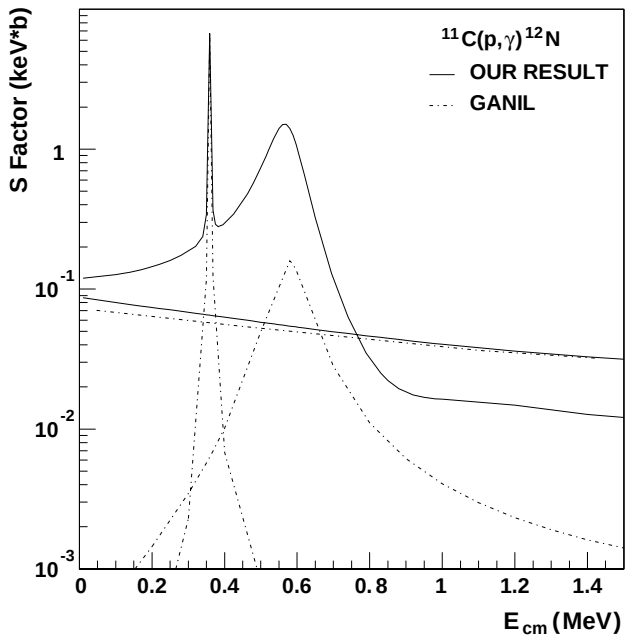

Fig. 2. The $^{11}\mathrm{C}(p,\gamma)^{12}\mathrm{N}$ S-factor *vs.* energy. The solid curves show our preliminary results for the total S-factor and the direct capture contribution alone. The dash-dotted curves show the various contributions determined in [9].

undergo nucleosynthesis via the *pp* chains or the triple-alpha process until heavier nuclei were produced to initiate the CNO cycle. Fuller *et al.* [7] have shown that, for super-massive first-generation stars, the standard *pp* chains that operate within our Sun generate too little energy and the triple-alpha reaction turns on too late to cause an explosion. Rather, such stars simply collapse to black holes. Thus, they would play no role in later galactic chemical evolution. More recently, Wiescher *et al.* [8] have noted that hot *pp* chains that were neglected in the earlier work may provide a path for super-massive first-generation stars to produce CNO nuclei at a lower temperature than required by the triple-alpha reaction. These CNO nuclei might then serve as seeds for further energy generation, stablizing the star against collapse long enough to permit an explosion to occur.

The $^{11}\mathrm{C}(p,\gamma)^{12}\mathrm{N}$ reaction is an important branch point in the hot *pp* chains. In massive objects, ^{11}C is produced efficiently at $T > 0.2$ GK via the $^7\mathrm{Be}(\alpha,\gamma)^{11}\mathrm{C}$ reaction. Its fate then depends on the competition between ^{11}C proton capture and beta-decay. If the density is sufficiently high that proton capture dominates, ^{11}C will provide a path to produce CNO nuclei. At lower densities, the path will be blocked by the $^{11}\mathrm{B}(p,3\alpha)$ reaction following ^{11}C beta-decay. At the interesting temperatures, both direct and resonant capture are expected to be significant. There have been two previous investigations of the $^{11}\mathrm{C}(p,\gamma)^{12}\mathrm{N}$ reaction, both using Coulomb breakup of ^{12}N [9,10], which have obtained conflicting results.

We have measured the $^{14}\mathrm{N}(^{11}\mathrm{C},^{12}\mathrm{N})^{13}\mathrm{C}$ reaction to determine the ANC for $^{11}\mathrm{C} + p \leftrightarrow {}^{12}\mathrm{N}$ and, in turn, the direct capture rate for $^{11}\mathrm{C}(p,\gamma)^{12}\mathrm{N}$ at astrophysical energies. The experiment used a ^{11}C radioactive beam, with an intensity of $\sim 4.2 \times 10^5$ particles/s at an energy of 10 MeV/u, incident on a 1.5 mg/cm^2 melamine target. The radioactive beam was produced with a ^{11}B beam from the Texas A&M K500 Superconducting Cyclotron in the reaction $^1\mathrm{H}(^{11}\mathrm{B},^{11}\mathrm{C})n$, and filtered by the recoil spectrometer MARS. Reaction products were measured by a pair of 5×5 cm^2 ΔE-E Si detector telescopes. Both ^{11}C elastic scattering off the melamine target and $^{14}\mathrm{N}(^{11}\mathrm{C},^{12}\mathrm{N})^{13}\mathrm{C}$ proton transfer reactions were observed simultaneously. The elastic scattering data have been used to verify the optical potentials for the radioactive nuclei that are used in the DWBA calculations of the proton transfer reaction.

Figure 2 shows our preliminary result for the direct capture contribution to the $^{11}\mathrm{C}(p,\gamma)^{12}\mathrm{N}$ astrophysical S-factor, as determined from our measured $^{11}\mathrm{C} + p \leftrightarrow {}^{12}\mathrm{N}$ ANCs. To determine the total S-factor, we also need to consider interference between the direct capture amplitude and resonance capture through the broad 2^- state at $E_R = 0.59$ MeV. The proton width of this state is known ($\Gamma_p = 0.118$ MeV), but its gamma width is uncertain [9,10]. In the R-matrix formalism, the proton width determines the structure of the resonant state in the external region, while our experimental ANC determines the asymptotic form of the ^{12}N ground state. Together, these are sufficient to calculate the external (channel) contribution to the gamma width of the resonance. For very loosely bound final states, this external contribution should dominate, thus allowing us to obtain an estimate of the gamma width. For a channel radius of 5 fm, the estimate is very close to a previous microscopic cluster model calculation by Descouvemont [11]. Figure 2 also shows our total S-factor. We conclude that the $^{11}\mathrm{C}(p,\gamma)^{12}\mathrm{N}$ reaction rate is

approximately twice as large as previously believed in the important temperature region.

3 ^{8}B halo radius from its ANC

Another nuclear property that clearly depends on the peripheral behavior of the nuclear wave function is halo structure. For example, measurements of the ^{8}B and ^{7}Be total interaction cross-sections and the ^{8}B single-proton removal cross-section indicate that [12,13]

$$\sigma_I(^8\mathrm{B}) \approx \sigma_I(^7\mathrm{Be}) + \sigma_{-1p}(^8\mathrm{B}), \qquad (2)$$

characteristic of a good single-nucleon halo. This leads to a very simple relationship between the root mean-square (rms) radius of the wave function of the last nucleon in ^{8}B and the overlap functions discussed above. After integrating over angles, the ^{8}B halo radius becomes [14,15]

$$r_\mathrm{h}^2 = \int_0^\infty I_\mathrm{g}^2(r) r^4 \mathrm{d}r + \int_0^\infty I_\mathrm{e}^2(r) r^4 \mathrm{d}r = r_\mathrm{g}^2 + r_\mathrm{e}^2, \qquad (3)$$

where $I_\mathrm{g}(r)$ and $I_\mathrm{e}(r)$ are the overlap functions arising from the parts of the ^{8}B ground-state wave function where the proton orbits the ground and first-excited states of the ^{7}Be core, respectively. The first term dominates. For it we can write, separating the contributions of the interior and the asymptotic regions,

$$r_\mathrm{g}^2 = \int_0^{R_N} I_\mathrm{g}^2(r) r^4 \mathrm{d}r + C_\mathrm{tot}^2 \int_{R_N}^\infty W^2(2\kappa r) r^2 \mathrm{d}r. \qquad (4)$$

In this, $C_\mathrm{tot}^2 = C_{p_{3/2}}^2 + C_{p_{1/2}}^2$ is the total ANC for ^{7}Be + $p \leftrightarrow {}^8$B and W is the Whittaker function. The contributions of the $p_{3/2}$ and $p_{1/2}$ orbitals to the exterior integral can be combined because they have the same behavior at large radii. Equation (4) demonstrates explicitly the dependence of the ^{8}B halo radius on its ANC.

Previously, as part of an experiment to determine the S-factor for $^7\mathrm{Be}(p,\gamma)^8\mathrm{B}$ from ANCs, we found $C_\mathrm{tot}^2 = 0.449 \pm 0.045$ fm^{-1} from measurements of two (^{7}Be,^{8}B) proton transfer reactions [16]. This allows us both to estimate the interior contribution to eq. (4) and to calculate the exterior contribution. We have considered a broad range of candidate single-particle overlap functions, obtained assuming Woods-Saxon, Gaussian, Morse, and square well potential shapes [15]. In each case, the tail of the overlap function was required to reproduce the experimentally determined ANC. With this constraint, we find essentially the same rms radius, independent of the choice of overlap function. This comes about because 85% of the contribution to r_g^2 comes from the region $R_N > 4$ fm, where the single-particle overlap functions already match the asymptotic Whittaker form. Furthermore, the matching constraint also fixes the small interior contribution to better than 2%. After including an estimate of the contribution to eq. (3) due to the ^{7}Be first-excited state, $r_\mathrm{e}^2 \approx 2.1$ fm^2, we find $r_\mathrm{h} = 4.20 \pm 0.22$ fm [15]. Most of this uncertainty is due to the experimental uncertainty in C_tot^2.

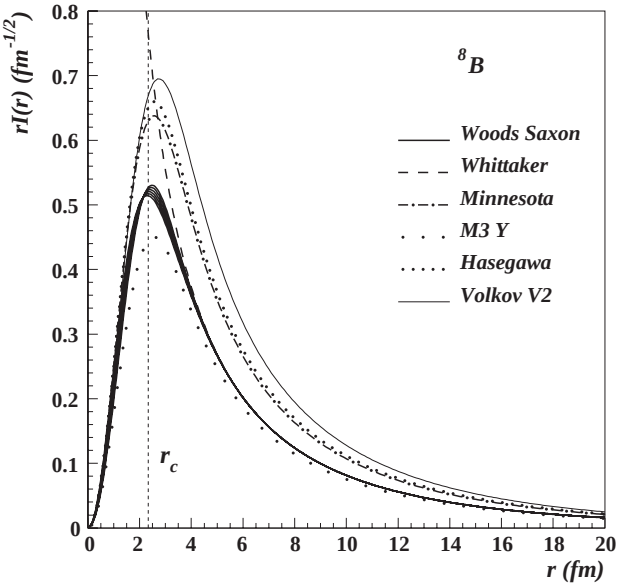

Fig. 3. ^{8}B overlap functions obtained with Woods-Saxon potentials are compared to a renormalized Whittaker function and to microscopic calculations assuming various effective interactions [14]. r_c is the radius of the ^{7}Be core.

Figure 3 shows typical overlap functions, which match the experimental ANC, that we obtained with Woods-Saxon potentials compared to microscopic self-consistent many-body calculations by Timofeyuk using various effective interactions [14]. All of the overlap functions have the same asymptotic shape as given by the Whittaker function, but only the M3Y interaction leads to an asymptotic magnitude close to ours. The others have far more strength in the asymptotic region and, therefore, do not match the measured ANC.

We can also compare calculations using our ^{8}B overlap functions [15] to experimental results for "traditional" halo observables, such as the longitudinal momentum distribution of core-like fragments in projectile breakup reactions and the one-proton removal cross-section. Using the Hansen model [17] to describe the breakup process, we find all of the overlap functions shown in fig. 3 predict similar widths for the ^{7}Be longitudinal momentum distribution in ^{8}B breakup on ^{9}Be at 41 MeV/u, close to that observed experimentally [18]. But only the overlap functions that match the experimental ANC reproduce the observed ^{8}B one-proton removal cross-section on ^{12}C at 40 MeV/u [19]. In contrast, the overlap functions in fig. 3 obtained with the Minnesota, Hasegawa, and Volkov effective interactions overpredict σ_{-1p} by factors of 2-3.

4 ^{8}B ANC from breakup and $^7\mathrm{Be}(\mathrm{p},\gamma)^8\mathrm{B}$

In the previous section, we showed that ANCs may be used to predict ^{8}B one-nucleon breakup cross-sections. This comes about because the breakup process is highly peripheral for loosely bound nuclei. But this is exactly the

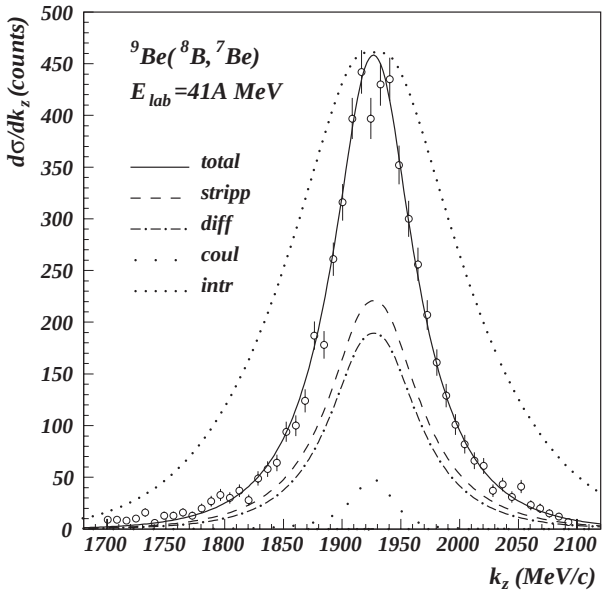

Fig. 4. Comparison of the calculated longitudinal momentum distribution for ^{7}Be fragments in ^{8}B breakup with experimental data [18]. The contributions from stripping, diffractive and Coulomb dissociation are also shown separately. The curve labeled "intr" shows the intrinsic distribution.

requirement for a reaction to be a good candidate for ANC measurements if we also have a reliable model to describe the breakup process itself. In fact, recent improvements in nuclear breakup reaction models now make a quantitative description possible for beam energies of tens to hundreds of MeV/u. Very recently, we have utilized these developments to make a new determination of the $^7\mathrm{Be} + p \leftrightarrow {}^8\mathrm{B}$ ANC [20]. This represents a new indirect way to determine the $^7\mathrm{Be}(p,\gamma)^8\mathrm{B}$ cross-section, which plays a key role in the solar-neutrino question [21].

Calculations have been done for ^{8}B one-proton breakup cross-sections on ^{12}C, ^{27}Al, ^{28}Si, ^{116}Sn, and ^{208}Pb at energies from 28 to 285 MeV/u [12,13]. To describe the breakup process, we adopted both the Hansen model [17] and an extended Glauber model, in the eikonal approximation with non-eikonal correction terms up to the second order. The Glauber model is similar to that developed by Bertsch *et al.* [22,23], and has been tested before on 23 different reactions in the *p-sd*-shell [24]. The loosely bound proton and the core, moving on an eikonal trajectory, interact independently with the target nucleus. For the proton-target interaction, we adopted that of Jeukenne, Lejeune and Mahaux (JLM) [25], in the updated version of Bauge *et al.* [26]. This interaction contains separate real and imaginary parts. For the target-core nucleus-nucleus interaction we used the double-folding procedure; the same JLM interaction was folded with Hartree-Fock nuclear-matter distributions for the core and target. The real and imaginary parts were then renormalized to match elastic scattering data. We find that the calculated ^{8}B one-proton breakup cross-sections are independent of the renormalization factor for the real part, and rather insentive to the renormalization factor for the imaginary part. Coulomb dissociation was treated in a perturbative method which, for low-Z targets, is equivalent with that of [27].

Figure 4 shows that the Glauber model provides an excellent description of the observed longitudinal momentum distribution for core-like fragments. We find consistent results for the ^{8}B ANC from the Glauber model calculations for ^{28}Si and ^{208}Pb targets, and also from the Hansen model calculations for all the targets. This consistency further validates the procedure. We conclude that $C^2_{\mathrm{tot}} = 0.437^{+0.041}_{-0.045}$ fm^{-1} for ^{8}B. This is in excellent agreement with our previous determination from (^{7}Be, ^{8}B) proton transfer reactions [16], but is sensitive to different systematic uncertainties. From this, we conclude $S_{17}(0) = 16.9^{+1.6}_{-1.7}$ eV b for $^7\mathrm{Be}(p,\gamma)^8\mathrm{B}$, in very good agreement with other recent direct and indirect determinations of the cross-section for this very important astrophysical reaction.

This work was supported in part by the US Department of Energy under Grant No. DE-FG03-93ER40773, by the US National Science Foundation under Grant No. INT-9909787, and by the Robert A. Welch Foundation.

References

1. A.M. Mukhamedzhanov *et al.*, Phys. Rev. C **56**, 1302 (1997).
2. R. Morlock *et al.*, Phys. Rev. Lett. **79**, 3837 (1997).
3. H.C. Chow, G.M. Griffith, T.H. Hall, Can. J. Phys. **53**, 1672 (1975).
4. C.A. Gagliardi *et al.*, Phys. Rev. C **59**, 1149 (1999).
5. A. Sattarov *et al.*, Phys. Rev. C **60**, 035801 (1999).
6. N. Imai *et al.*, Nucl. Phys. A **688**, 281c (2001).
7. G.M. Fuller, S.E. Woosley, T.A. Weaver, Astrophys. J. **307**, 675 (1986).
8. M. Wiescher *et al.*, Astrophys. J. **343**, 352 (1989).
9. A. Lefebvre *et al.*, Nucl. Phys. A **592**, 69 (1995).
10. T. Motobayashi, *Proceedings of the 2nd International Conference on Exotic Nuclei Atomic Masses, ENAM98*, edited by B.M. Sherrill, D.J. Morrisey, C.N. Davids, AIP Conf. Proc. **455**, 882 (1998); T. Minemura *et al.*, *Coulomb dissociation of* ^{12}N *and* ^{13}O, poster contribution, to be published in *Exotic Nuclei and Atomic Masses* (Springer-Verlag, Heidelberg, 2002).
11. P. Descouvemont, Nucl. Phys. A **646**, 261 (1999).
12. F. Negoita *et al.*, Phys. Rev. C **54**, 1787 (1996).
13. B. Blank *et al.*, Nucl. Phys. A **624**, 242 (1997).
14. N.K. Timofeyuk, Nucl. Phys. A **632**, 19 (1998).
15. F. Carstoiu *et al.*, Phys. Rev. C **63**, 054310 (2001).
16. A. Azhari *et al.*, Phys. Rev. C **63**, 055803 (2001).
17. P.G. Hansen, Phys. Rev. Lett. **77**, 1016 (1996).
18. J.H. Kelley *et al.*, Phys. Rev. Lett. **77**, 5020 (1996).
19. I. Pecina *et al.*, Phys. Rev. C **52**, 191 (1995).
20. L. Trache *et al.*, Phys. Rev. Lett. **87**, 271102 (2002).
21. E.G. Adelberger *et al.*, Rev. Mod. Phys. **70**, 1265 (1998).
22. G. Bertsch, H. Esbensen, A. Sustich, Phys. Rev. C **42**, 758 (1990).

23. K. Hencken, G. Bertsch, H. Esbensen, Phys. Rev. C **54**, 3043 (1996).
24. E. Sauvan *et al.*, Phys. Lett. B **491**, 1 (2000).
25. J.P. Jeukenne, A. Lejeune, C. Mahaux, Phys. Rev. C **16**, 80 (1977).
26. E. Bauge, J.P. Delaroche, M. Girod, Phys. Rev. C **58**, 1118 (1998).
27. C. Bertulani, G. Baur, Nucl. Phys. A **480**, 615 (1988).